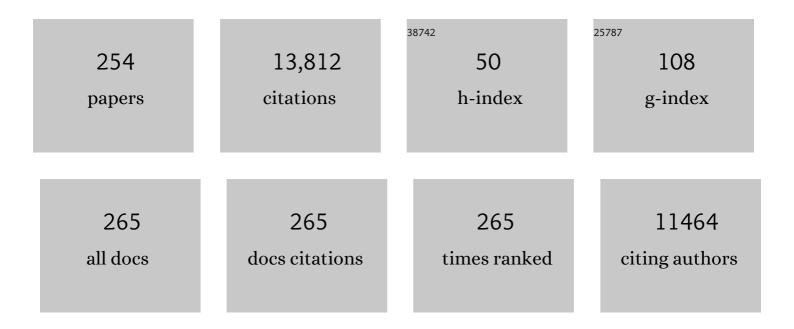
Chuan-Chou Shen

List of Publications by Year in descending order

Source: https://exaly.com/author-pdf/8537617/publications.pdf Version: 2024-02-01



#	Article	IF	CITATIONS
1	A High-Resolution Absolute-Dated Late Pleistocene Monsoon Record from Hulu Cave, China. Science, 2001, 294, 2345-2348.	12.6	2,594
2	Improvements in 230Th dating, 230Th and 234U half-life values, and U–Th isotopic measurements by multi-collector inductively coupled plasma mass spectrometry. Earth and Planetary Science Letters, 2013, 371-372, 82-91.	4.4	1,007
3	Wet periods in northeastern Brazil over the past 210 kyr linked to distant climate anomalies. Nature, 2004, 432, 740-743.	27.8	698
4	Uranium and thorium isotopic and concentration measurements by magnetic sector inductively coupled plasma mass spectrometry. Chemical Geology, 2002, 185, 165-178.	3.3	395
5	Neandertal roots: Cranial and chronological evidence from Sima de los Huesos. Science, 2014, 344, 1358-1363.	12.6	356
6	Earthquake Supercycles Inferred from Sea-Level Changes Recorded in the Corals of West Sumatra. Science, 2008, 322, 1674-1678.	12.6	323
7	A late Middle Pleistocene Denisovan mandible from the Tibetan Plateau. Nature, 2019, 569, 409-412.	27.8	302
8	High-precision and high-resolution carbonate 230Th dating by MC-ICP-MS with SEM protocols. Geochimica Et Cosmochimica Acta, 2012, 99, 71-86.	3.9	277
9	Variability of stalagmite-inferred Indian monsoon precipitation over the past 252,000 y. Proceedings of the United States of America, 2015, 112, 2954-2959.	7.1	233
10	Organ biodistribution, clearance, and genotoxicity of orally administered zinc oxide nanoparticles in mice. Nanotoxicology, 2012, 6, 746-756.	3.0	206
11	The calibration of D[Sr/Ca]versus sea surface temperature relationship for Porites corals. Geochimica Et Cosmochimica Acta, 1996, 60, 3849-3858.	3.9	197
12	Archaea and bacteria with surprising microdiversity show shifts in dominance over 1,000-year time scales in hydrothermal chimneys. Proceedings of the National Academy of Sciences of the United States of America, 2010, 107, 1612-1617.	7.1	181
13	Measurement of Attogram Quantities of231Pa in Dissolved and Particulate Fractions of Seawater by Isotope Dilution Thermal Ionization Mass Spectroscopy. Analytical Chemistry, 2003, 75, 1075-1079.	6.5	168
14	Variation of initial 230Th/232Th and limits of high precision U–Th dating of shallow-water corals. Geochimica Et Cosmochimica Acta, 2008, 72, 4201-4223.	3.9	162
15	Recent enhancement of central Pacific El Niño variability relative to last eight centuries. Nature Communications, 2017, 8, 15386.	12.8	126
16	High-resolution absolute-dated Indian Monsoon record between 53 and 36 ka from Xiaobailong Cave, southwestern China. Geology, 2006, 34, 621.	4.4	125
17	Obliquity pacing of the western Pacific Intertropical Convergence Zone over the past 282,000 years. Nature Communications, 2015, 6, 10018.	12.8	124
18	Improving coral-base paleoclimate reconstructions by replicating 350years of coral Sr/Ca variations. Palaeogeography, Palaeoclimatology, Palaeoecology, 2013, 373, 6-24.	2.3	122

#	Article	IF	CITATIONS
19	Comparison of the Quaternary travertine sites in the Denizli extensional basin based on their depositional and geochemical data. Sedimentary Geology, 2013, 294, 179-204.	2.1	119
20	Coupling of Indo-Pacific climate variability over the last millennium. Nature, 2020, 579, 385-392.	27.8	116
21	Huge erratic boulders in Tonga deposited by a prehistoric tsunami. Geology, 2009, 37, 131-134.	4.4	111
22	Mg/Ca ratios of twoGlobigerinoides ruber(white) morphotypes: Implications for reconstructing past tropical/subtropical surface water conditions. Geochemistry, Geophysics, Geosystems, 2005, 6, n/a-n/a.	2.5	106
23	Coral evidence for earthquake recurrence and an A.D. 1390–1455 cluster at the south end of the 2004 Aceh–Andaman rupture. Journal of Geophysical Research, 2010, 115, .	3.3	96
24	Accelerated drawdown of meridional overturning in the late-glacial Atlantic triggered by transient pre-H event freshwater perturbation. Geophysical Research Letters, 2006, 33, .	4.0	89
25	Oxygen and carbon isotopic systematics of aragonite speleothems and water in Furong Cave, Chongqing, China. Geochimica Et Cosmochimica Acta, 2011, 75, 4140-4156.	3.9	87
26	On the influence of sea level and monsoon climate on the southern South China Sea freshwater budget over the last 22,000 years. Quaternary Science Reviews, 2006, 25, 1475-1488.	3.0	84
27	Dissolved and particulate 231 Pa and 230 Th in the Atlantic Ocean: constraints on intermediate/deep water age, boundary scavenging, and 231 Pa/ 230 Th fractionation. Earth and Planetary Science Letters, 2002, 203, 999-1014.	4.4	83
28	Uranium-series coral ages from the US Atlantic Coastal Plain–the "80ka problem―revisited. Quaternary International, 2004, 120, 3-14.	1.5	83
29	Reconciliation of hydroclimate sequences from the Chinese Loess Plateau and low-latitude East Asian Summer Monsoon regions over the past 14,500years. Palaeogeography, Palaeoclimatology, Palaeoecology, 2015, 435, 127-135.	2.3	82
30	Late Bronze Age climate change and the destruction of the Mycenaean Palace of Nestor at Pylos. PLoS ONE, 2017, 12, e0189447.	2.5	79
31	Progressive aridification in East Africa over the last half million years and implications for human evolution. Proceedings of the National Academy of Sciences of the United States of America, 2018, 115, 11174-11179.	7.1	77
32	Time-varying interseismic strain rates and similar seismic ruptures on the Nias–Simeulue patch of the Sunda megathrust. Quaternary Science Reviews, 2015, 122, 258-281.	3.0	74
33	Rainfall variations in central Indo-Pacific over the past 2,700 y. Proceedings of the National Academy of Sciences of the United States of America, 2019, 116, 17201-17206.	7.1	73
34	Decreasing monsoon precipitation in southwest China during the last 240Âyears associated with the warming of tropical ocean. Climate Dynamics, 2017, 48, 1769-1778.	3.8	72
35	Persistent termini of 2004―and 2005â€ŀike ruptures of the Sunda megathrust. Journal of Geophysical Research, 2012, 117, .	3.3	70
36	A reconstruction of sea surface temperature variability in the southeastern Gulf of Mexico from 1734 to 2008 C.E. using crossâ€dated Sr/Ca records from the coral <i>Siderastrea siderea</i> . Paleoceanography, 2014, 29, 403-422.	3.0	70

#	Article	IF	CITATIONS
37	Sea surface temperature variability in the southwest tropical Pacific since AD 1649. Nature Climate Change, 2012, 2, 799-804.	18.8	69
38	U–Th systematics and 230Th ages of carbonate chimneys at the Lost City Hydrothermal Field. Geochimica Et Cosmochimica Acta, 2011, 75, 1869-1888.	3.9	68
39	Radiocarbon Dating of Deep-Sea Corals. Radiocarbon, 2002, 44, 567-580.	1.8	65
40	The Holocene Pulleniatina Minimum Event revisited: Geochemical and faunal evidence from the Okinawa Trough and upper reaches of the Kuroshio current. Marine Micropaleontology, 2006, 59, 153-170.	1.2	60
41	Cyclic precipitation variation on the western Loess Plateau of China during the past four centuries. Scientific Reports, 2014, 4, 6381.	3.3	60
42	Earthquake supercycles on the Mentawai segment of the Sunda megathrust in the seventeenth century and earlier. Journal of Geophysical Research: Solid Earth, 2017, 122, 642-676.	3.4	59
43	Hydrothermal fluids circulation and travertine deposition in an active tectonic setting: Insights from the Kamara geothermal area (western Anatolia, Turkey). Tectonophysics, 2016, 680, 211-232.	2.2	58
44	The earliest modern Homo sapiens in China?. Journal of Human Evolution, 2016, 101, 101-104.	2.6	58
45	An evaluation of quantitative reconstruction of past precipitation records using coral skeletal Sr/Ca and δ180 data. Earth and Planetary Science Letters, 2005, 237, 370-386.	4.4	57
46	East Asian monsoon evolution and reconciliation of climate records from Japan and Greenland during the last deglaciation. Quaternary Science Reviews, 2010, 29, 3327-3335.	3.0	57
47	The δ18O and δ13C records in an aragonite stalagmite from Furong Cave, Chongqing, China: A-2000-year record of monsoonal climate. Journal of Asian Earth Sciences, 2011, 40, 1121-1130.	2.3	56
48	Early-Holocene monsoon instability and climatic optimum recorded by Chinese stalagmites. Holocene, 2019, 29, 1059-1067.	1.7	56
49	Gradual onset and recovery of the Younger Dryas abrupt climate event in the tropics. Nature Communications, 2015, 6, 8061.	12.8	55
50	Multidecadal rainfall variability in South Pacific Convergence Zone as revealed by stalagmite geochemistry. Geology, 2013, 41, 1143-1146.	4.4	51
51	High-resolution speleothem record of precipitation from the Yucatan Peninsula spanning the Maya Preclassic Period. Global and Planetary Change, 2016, 138, 93-102.	3.5	49
52	Rupture and variable coupling behavior of the Mentawai segment of the Sunda megathrust during the supercycle culmination of 1797 to 1833. Journal of Geophysical Research: Solid Earth, 2014, 119, 7258-7287.	3.4	47
53	Evidence for solar cycles in a late Holocene speleothem record from Dongge Cave, China. Scientific Reports, 2014, 4, 5159.	3.3	47
54	Penultimate predecessors of the 2004 Indian Ocean tsunami in Aceh, Sumatra: Stratigraphic, archeological, and historical evidence. Journal of Geophysical Research: Solid Earth, 2015, 120, 308-325.	3.4	45

#	Article	IF	CITATIONS
55	A snapshot of climate variability at Tahiti at 9.5 ka using a fossil coral from IODP Expedition 310. Geochemistry, Geophysics, Geosystems, 2010, 11, .	2.5	44
56	Sedimentological and geochemical characteristics of a fluvial travertine: A case from the eastern Mediterranean region. Sedimentology, 2014, 61, 291-318.	3.1	44
57	Heinrich event 4 and Dansgaard/Oeschger events 5–10 recorded by high-resolution speleothem oxygen isotope data from central China. Quaternary Research, 2014, 82, 394-404.	1.7	44
58	Thallium dispersal and contamination in surface sediments from South China and its source identification. Environmental Pollution, 2016, 213, 878-887.	7.5	44
59	Deglacial variations of Sr and 87Sr/86Sr ratio recorded by a stalagmite from Central China and their association with past climate and environment. Chemical Geology, 2009, 268, 233-247.	3.3	42
60	Permanent upper plate deformation in western Myanmar during the great 1762 earthquake: Implications for neotectonic behavior of the northern Sunda megathrust. Journal of Geophysical Research: Solid Earth, 2013, 118, 1277-1303.	3.4	42
61	Quaternary history of the Lake Magadi Basin, southern Kenya Rift: Tectonic and climatic controls. Palaeogeography, Palaeoclimatology, Palaeoecology, 2019, 518, 97-118.	2.3	42
62	Stalagmite-inferred Holocene precipitation in northern Guizhou Province, China, and asynchronous termination of the Climatic Optimum in the Asian monsoon territory. Science Bulletin, 2012, 57, 795-801.	1.7	41
63	Testing the annual nature of speleothem banding. Scientific Reports, 2013, 3, 2633.	3.3	41
64	Lead Isotope Characterization of Petroleum Fuels in Taipei, Taiwan. International Journal of Environmental Research and Public Health, 2015, 12, 4602-4616.	2.6	41
65	Recrystallization-induced oxygen isotope changes in inclusion-hosted water of speleothems – Paleoclimatological implications. Quaternary International, 2016, 415, 25-32.	1.5	41
66	Geochemical transfer and preliminary health risk assessment of thallium in a riverine system in the Pearl River Basin, South China. Journal of Geochemical Exploration, 2017, 176, 64-75.	3.2	41
67	Holocene stalagmite oxygen isotopic record from the Japan Sea side of the Japanese Islands, as a new proxy of the East Asian winter monsoon. Quaternary Science Reviews, 2013, 75, 150-160.	3.0	40
68	New dating evidence of the early presence of hominins in Southern Europe. Scientific Reports, 2017, 7, 10074.	3.3	40
69	High-resolution mid-Holocene Indian Summer Monsoon recorded in a stalagmite from the Kotumsar Cave, Central India. Quaternary International, 2018, 479, 19-24.	1.5	40
70	Geochemical and U-Th isotopic insights on uranium enrichment in reservoir sediments. Journal of Hazardous Materials, 2021, 414, 125466.	12.4	40
71	Three thousand years of extreme rainfall events recorded in stalagmites from Spring Valley Caverns, Minnesota. Earth and Planetary Science Letters, 2010, 300, 46-54.	4.4	38
72	Climate and environmental changes during the past millennium in central western Guizhou, China as recorded by Stalagmite ZJD-21. Journal of Asian Earth Sciences, 2011, 40, 1111-1120.	2.3	38

#	Article	IF	CITATIONS
73	Growth of a Pleistocene giant carbonate vein and nearby thermogene travertine deposits at Semproniano, southern Tuscany, Italy: Estimate of CO2 leakage. Tectonophysics, 2016, 690, 219-239.	2.2	38
74	Constraints on deep water age and particle flux in the equatorial and South Atlantic Ocean based on seawater231Pa and230Th data. Geophysical Research Letters, 2001, 28, 3437-3440.	4.0	37
75	Rapid retreat of the East Asian summer monsoon in the middle Holocene and a millennial weak monsoon interval at 9â€ka in northern China. Journal of Asian Earth Sciences, 2018, 151, 31-39.	2.3	37
76	Speleothem based 1000-year high resolution record of Indian monsoon variability during the last deglaciation. Palaeogeography, Palaeoclimatology, Palaeoecology, 2014, 395, 1-8.	2.3	36
77	A Chinese cave links climate change, social impacts and human adaptation over the last 500 years. Scientific Reports, 2015, 5, 12284.	3.3	36
78	Stable isotope compositions of speleothems from the last interglacial – Spatial patterns of climate fluctuations in Europe. Quaternary Science Reviews, 2017, 161, 68-80.	3.0	36
79	Calcite veining and feeding conduits in a hydrothermal system: Insights from a natural section across the Pleistocene GA¶lemezli travertine depositional system (western Anatolia, Turkey). Sedimentary Geology, 2018, 364, 180-203.	2.1	36
80	231Pa and 230Th in surface sediments of the Arctic Ocean: Implications for 231Pa/230Th fractionation, boundary scavenging, and advective export. Earth and Planetary Science Letters, 2005, 234, 235-248.	4.4	35
81	Bronze Age volcanic event recorded in stalagmites by combined isotope and trace element studies. Rapid Communications in Mass Spectrometry, 2009, 23, 801-808.	1.5	35
82	Stalagmite-inferred variability of the Asian summer monsoon during the penultimate glacial–interglacial period. Climate of the Past, 2014, 10, 1211-1219.	3.4	33
83	Trace-element variations in an annually layered stalagmite as recorders of climatic changes and anthropogenic pollution in Central China. Quaternary Research, 2014, 81, 181-188.	1.7	33
84	Refining temperature reconstructions with the Atlantic coral Siderastrea siderea. Palaeogeography, Palaeoclimatology, Palaeoecology, 2016, 462, 1-15.	2.3	33
85	Key travertine tectofacies for neotectonics and palaeoseismicity reconstruction: effects of hydrothermal overpressured fluid injection. Journal of the Geological Society, 2017, 174, 679-699.	2.1	33
86	Holocene Solar Activity Imprint on Centennial―to Multidecadal‧cale Hydroclimatic Oscillations in Arid Central Asia. Journal of Geophysical Research D: Atmospheres, 2019, 124, 2562-2573.	3.3	33
87	Mysterious abrupt carbon-14 increase in coral contributed by a comet. Scientific Reports, 2014, 4, 3728.	3.3	32
88	Variation of the Asian summer monsoon since the last glacial-interglacial recorded in a stalagmite from southwest China. Quaternary Science Reviews, 2020, 234, 106261.	3.0	32
89	Natal origin of Pacific bluefin tuna Thunnus orientalis inferred from otolith oxygen isotope composition. Marine Ecology - Progress Series, 2010, 420, 207-219.	1.9	32
90	High precision glacial–interglacial benthic foraminiferal Sr/Ca records from the eastern equatorial Atlantic Ocean and Caribbean Sea. Earth and Planetary Science Letters, 2001, 190, 197-209.	4.4	31

#	Article	IF	CITATIONS
91	Oceanic magmatism in sedimentary basins of the northern Gulf of California rift. Bulletin of the Geological Society of America, 2013, 125, 1833-1850.	3.3	31
92	Climate significance of speleothem l´180 from central China on decadal timescale. Journal of Asian Earth Sciences, 2015, 106, 150-155.	2.3	31
93	Travertine deposits constraining transfer zone neotectonics in geothermal areas: An example from the inner Northern Apennines (Bagno Vignoni-Val d'Orcia area, Italy). Geothermics, 2020, 85, 101763.	3.4	31
94	Coral record of reduced El Nino activity in the early 15th to middle 17th centuries. Geology, 2013, 41, 51-54.	4.4	30
95	Recent 121â€year variability of western boundary upwelling in the northern South China Sea. Geophysical Research Letters, 2013, 40, 3180-3183.	4.0	30
96	Annually-resolved coral skeletal δ138/134Ba records: A new proxy for oceanic Ba cycling. Geochimica Et Cosmochimica Acta, 2019, 247, 27-39.	3.9	30
97	Changes in climate and vegetation of central Guizhou in southwest China since the last glacial reflected by stalagmite records from Yelang Cave. Journal of Asian Earth Sciences, 2015, 114, 549-561.	2.3	29
98	Acceleration of modern acidification in the South China Sea driven by anthropogenic CO2. Scientific Reports, 2014, 4, 5148.	3.3	29
99	Potential influence of temperature changes in the Southern Hemisphere on the evolution of the Asian summer monsoon during the last glacial period. Quaternary International, 2016, 392, 239-250.	1.5	29
100	Uranium-Series Dating of Speleothems: Current Techniques, Limits, & Applications. , 2004, , 177-197.		29
101	Application of U/Th and 40Ar/39Ar Dating to Orgnac 3, a Late Acheulean and Early Middle Palaeolithic Site in Ardèche, France. PLoS ONE, 2013, 8, e82394.	2.5	28
102	Precise oxygen and hydrogen isotope determination in nanoliter quantities of speleothem inclusion water by cavity ring-down spectroscopic techniques. Geochimica Et Cosmochimica Acta, 2016, 172, 159-176.	3.9	28
103	Dynamic millennialâ€scale climate changes in the northwestern Pacific over the past 40,000 years. Geophysical Research Letters, 2010, 37, .	4.0	27
104	Radiocarbon dating of residual organic matter in travertine formed along the Yumoto Fault in Oga Peninsula, northeast Japan: Implications for long-term hot spring activity under the influence of earthquakes. Sedimentary Geology, 2012, 243-244, 181-190.	2.1	27
105	Neodymium isotopic composition and concentration in the Southwest Pacific Ocean. Geochemical Journal, 2013, 47, 409-422.	1.0	27
106	Persistent decadal-scale rainfall variability in the tropical South Pacific Convergence Zone through the past six centuries. Climate of the Past, 2014, 10, 1319-1332.	3.4	27
107	Great flood in the middle-lower Yellow River reaches at 4000 a BP inferred from accurately-dated stalagmite records. Science Bulletin, 2018, 63, 206-208.	9.0	27
108	A long record of MIS 7 and MIS 5 climate and environment from a western Mediterranean speleothem (SW Sardinia, Italy). Quaternary Science Reviews, 2019, 220, 230-243.	3.0	27

#	Article	IF	CITATIONS
109	Decadal changes in the mid-depth water mass dynamic of the Northeastern Atlantic margin (Bay of) Tj ETQq1	1 0.784314 4.4	rgBT /Overlo
110	Natural attrition and growth frequency variations of stalagmites in southwest Sulawesi over the past 530,000 years. Palaeogeography, Palaeoclimatology, Palaeoecology, 2016, 441, 823-833.	2.3	26
111	Stalagmite-inferred centennial variability of the Asian summer monsoon in southwest China between 58 and 79Âka BP. Quaternary Science Reviews, 2017, 160, 1-12.	3.0	26
112	Mid-Holocene climate conditions and moisture source variations based on stable H, C and O isotope compositions of speleothems in Hungary. Quaternary International, 2013, 293, 150-156.	1.5	25
113	Surface Sediment Contamination by Uranium Mining/Milling Activities in South China. Clean - Soil, Air, Water, 2015, 43, 414-420.	1.1	24
114	Inconsistency between records of δ ¹⁸ O and trace element ratios from stalagmites: Evidence for increasing mid–late Holocene moisture in arid central Asia. Holocene, 2020, 30, 369-379.	1.7	24
115	High precision measurements of Mg/Ca and Sr/Ca ratios in carbonates by cold plasma inductively coupled plasma quadrupole mass spectrometry. Chemical Geology, 2007, 236, 339-349.	3.3	23
116	U-series disequilibrium in young Tengchong volcanics: Recycling of mature clay sediments or mudstones into the SE Tibetan mantle. Lithos, 2014, 192-195, 132-141.	1.4	23
117	Nonlinear climatic sensitivity to greenhouse gases over past 4 glacial/interglacial cycles. Scientific Reports, 2017, 7, 4626.	3.3	23
118	Precession and atmospheric CO2 modulated variability of sea ice in the central Okhotsk Sea since 130,000 years ago. Earth and Planetary Science Letters, 2018, 488, 36-45.	4.4	23
119	Neodymium concentration and isotopic composition distributions in the southwestern Indian Ocean and the Indian sector of the Southern Ocean. Chemical Geology, 2019, 511, 190-203.	3.3	23
120	Sea-level rise and coral-reef development of Northwestern Luzon since 9.9ka. Palaeogeography, Palaeoclimatology, Palaeoecology, 2010, 292, 465-473.	2.3	22
121	Prior calcite precipitation and source mixing process influence Sr/Ca, Ba/Ca and 87Sr/86Sr of a stalagmite developed in southwestern Japan during 18.0‒4.5ka. Chemical Geology, 2013, 347, 190-198.	3.3	21
122	Quantitative temperature reconstruction based on growth rate of annually-layered stalagmite: a case study from central China. Quaternary Science Reviews, 2013, 72, 137-145.	3.0	21
123	Precisely dated multidecadally resolved Asian summer monsoon dynamics 113.5–86.6 thousand years ago. Quaternary Science Reviews, 2016, 143, 1-12.	3.0	21
124	Multi-scale Holocene Asian monsoon variability deduced from a twin-stalagmite record in southwestern China. Quaternary Research, 2016, 86, 34-44.	1.7	21
125	A penultimate glacial climate record from southern Hungary. Journal of Quaternary Science, 2017, 32, 946-956.	2.1	21
126	Occurrence of 1Âka-old corals on an uplifted reef terrace in west Luzon, Philippines: Implications for a prehistoric extreme wave event in the South China Sea region. Geoscience Letters, 2017, 4, .	3.3	21

#	Article	IF	CITATIONS
127	Quaternary hinterland evolution of the active Banda Arc: Surface uplift and neotectonic deformation recorded by coral terraces at Kisar, Indonesia. Journal of Asian Earth Sciences, 2013, 73, 149-161.	2.3	20
128	Replicated stalagmite-inferred centennial-to decadal-scale monsoon precipitation variability in southwest China since the mid Holocene. Holocene, 2013, 23, 841-849.	1.7	19
129	Reconstructing surface ocean circulation with 129 I time series records from corals. Journal of Environmental Radioactivity, 2016, 165, 144-150.	1.7	19
130	Synchronous precipitation reduction in the American Tropics associated with Heinrich 2. Scientific Reports, 2017, 7, 11216.	3.3	19
131	Reconstruction of Indian monsoon precipitation variability between 4.0 and 1.6Âka BP using speleothem δ180 records from the Central Lesser Himalaya, India. Arabian Journal of Geosciences, 2017, 10, 1.	1.3	19
132	Asian monsoon dynamics at Dansgaard/Oeschger events 14–8 and Heinrich events 5–4 in northern China. Quaternary Geochronology, 2018, 47, 72-80.	1.4	19
133	Decoupling of stalagmite-derived Asian summer monsoon records from North Atlantic temperature change during marine oxygen isotope stage 5d. Quaternary Research, 2008, 70, 315-321.	1.7	18
134	Interannual variation of rare earth element abundances in corals from northern coast of the South China Sea and its relation with sea-level change and human activities. Marine Environmental Research, 2011, 71, 62-69.	2.5	18
135	Variations of monsoonal rain and vegetation during the past millennium in Tiangui Mountain, North China reflected by stalagmite δ18O and δ13C records from Zhenzhu Cave. Quaternary International, 2017, 447, 89-101.	1.5	18
136	Quantification of paleo-aquifer changes using clumped isotopes in subaqueous carbonate speleothems. Chemical Geology, 2018, 493, 246-257.	3.3	18
137	Experimental evaluation of oxygen isotopic exchange between inclusion water and host calcite in speleothems. Climate of the Past, 2020, 16, 17-27.	3.4	18
138	An ancient shallow slip event on the Mentawai segment of the Sunda megathrust, Sumatra. Journal of Geophysical Research, 2012, 117, .	3.3	17
139	Decoupling of the East Asian summer monsoon and Indian summer monsoon between 20 and 17 ka. Quaternary Research, 2014, 82, 146-153.	1.7	17
140	Variable Holocene deformation above a shallow subduction zone extremely close to the trench. Nature Communications, 2015, 6, 7607.	12.8	17
141	Hypogenic speleogenesis, late stage epigenic overprinting and condensation-corrosion in a complex cave system in relation to landscape evolution (Toirano, Liguria, Italy). Geomorphology, 2021, 376, 107561.	2.6	17
142	Determination of element/Ca ratios in foraminifera and corals using cold- and hot-plasma techniques in inductively coupled plasma sector field mass spectrometry. Journal of Asian Earth Sciences, 2014, 81, 115-122.	2.3	16
143	Late Pleistocene zircon ages for intracaldera domes at Gölcük (Isparta, Turkey). Journal of Volcanology and Geothermal Research, 2014, 286, 24-29.	2.1	16
144	Evolution of the Asian summer monsoon during Dansgaard/Oeschger events 13–17 recorded in a stalagmite constrained by high-precision chronology from southwest China. Quaternary Research, 2017, 88, 121-128.	1.7	16

#	Article	IF	CITATIONS
145	Multidecadally resolved polarity oscillations during a geomagnetic excursion. Proceedings of the National Academy of Sciences of the United States of America, 2018, 115, 8913-8918.	7.1	16
146	Magmatic-like fluid source of the Chingshui geothermal field, NE Taiwan evidenced by carbonate clumped-isotope paleothermometry. Journal of Asian Earth Sciences, 2017, 149, 124-133.	2.3	15
147	Improved analytical techniques of sulfur isotopic composition in nanomole quantities by MC-ICP-MS. Analytica Chimica Acta, 2017, 988, 34-40.	5.4	15
148	Upper-plate splay fault earthquakes along the Arakan subduction belt recorded by uplifted coral microatolls on northern Ramree Island, western Myanmar (Burma). Earth and Planetary Science Letters, 2018, 484, 241-252.	4.4	15
149	Speleothems and pine trees as sensitive indicators of environmental pollution $\hat{a} \in A$ case study of the effect of uranium-ore mining in Hungary. Applied Geochemistry, 2011, 26, 666-678.	3.0	14
150	U-series dating of co-seismic gypsum and submarine paleoseismology of active faults in Northern Chile (23°S). Tectonophysics, 2011, 497, 34-44.	2.2	14
151	Persistent sea surface temperature and declined sea surface salinity in the northwestern tropical Pacific over the past 7500years. Journal of Asian Earth Sciences, 2013, 66, 234-239.	2.3	14
152	The climate reconstruction in Shandong Peninsula, northern China, during the last millennium based on stalagmite laminae together with a comparison to <i>l´</i> ¹⁸ O. Climate of the Past, 2016, 12, 871-881.	3.4	14
153	High-resolution reconstruction of Indian summer monsoon during the BÃ,lling-Allerà d from a central Indian stalagmite. Palaeogeography, Palaeoclimatology, Palaeoecology, 2019, 514, 567-576.	2.3	14
154	Genesis and diagenesis of travertine, Futamata hot spring, Japan. Sedimentary Geology, 2020, 405, 105706.	2.1	14
155	Geothermal Fluid Variation Recorded by Banded Ca-Carbonate Veins in a Fault-Related, Fissure Ridge-Type Travertine Depositional System (Iano, southern Tuscany, Italy). Geofluids, 2021, 2021, 1-28.	0.7	14
156	Karst hydrological changes during the Late-Holocene in Southwestern China. Quaternary Science Reviews, 2021, 258, 106865.	3.0	14
157	A novel method for tracing coastal water masses using Sr/Ca ratios and salinity in Nanwan Bay, southern Taiwan. Estuarine, Coastal and Shelf Science, 2005, 65, 135-142.	2.1	13
158	Millennial meridional dynamics of the Indo-Pacific Warm Pool during the last termination. Climate of the Past, 2014, 10, 2253-2261.	3.4	13
159	An insight into the western Pacific wintertime moisture sources using dual water vapor isotopes. Journal of Hydrology, 2017, 547, 111-123.	5.4	13
160	High-resolution δ180 and δ13C records of an AMS 14C and 230Th/U dated stalagmite from Xinya Cave in Chongqing: Climate and vegetation change during the late Holocene. Quaternary International, 2017, 447, 75-88.	1.5	13
161	North Atlantic influences on climate conditions in East-Central Europe in the late Holocene reflected by flowstone compositions. Quaternary International, 2019, 512, 99-112.	1.5	13
162	Spatial-Temporal Evolution of Extensional Faulting and Fluid Circulation in the Amatrice Basin (Central Apennines, Italy) During the Pleistocene. Frontiers in Earth Science, 2020, 8, .	1.8	13

#	Article	IF	CITATIONS
163	Discharge of deeply rooted fluids from submarine mud volcanism in the Taiwan accretionary prism. Scientific Reports, 2020, 10, 381.	3.3	13
164	Hydroclimate variability of central Indo-Pacific region during the Holocene. Quaternary Science Reviews, 2021, 253, 106779.	3.0	13
165	A million year vegetation history and palaeoenvironmental record from the Lake Magadi Basin, Kenya Rift Valley. Palaeogeography, Palaeoclimatology, Palaeoecology, 2021, 567, 110247.	2.3	13
166	High precise dating on the variation of the Asian summer monsoon since 37Âka BP. Scientific Reports, 2021, 11, 9375.	3.3	13
167	Abrupt Southern Great Plains thunderstorm shifts linked to glacial climate variability. Nature Geoscience, 2021, 14, 396-401.	12.9	13
168	Measurements of Natural Carbonate Rare Earth Elements in Femtogram Quantities by Inductive Coupled Plasma Sector Field Mass Spectrometry. Analytical Chemistry, 2011, 83, 6842-6848.	6.5	12
169	Temperature and seawater isotopic controls on two stalagmite records since 83 ka from maritime Japan. Quaternary Science Reviews, 2018, 192, 47-58.	3.0	12
170	Moderate zooxanthellate coral growth rates in the lower photic zone. Coral Reefs, 2020, 39, 1273-1284.	2.2	12
171	A Century of Reduced ENSO Variability During the Medieval Climate Anomaly. Paleoceanography and Paleoclimatology, 2020, 35, e2019PA003742.	2.9	12
172	Little Ice Age climate changes in Southwest China from a stalagmite δ180 record. Palaeogeography, Palaeoclimatology, Palaeoecology, 2021, 562, 110167.	2.3	12
173	Insights from barium variability in a Siderastrea siderea coral in the northwestern Gulf of Mexico. Marine Pollution Bulletin, 2021, 173, 112930.	5.0	12
174	Sr thermometer for Porites corals. Little need to measure Ca?. Geochemical Journal, 1999, 33, 351-354.	1.0	11
175	Rare earth elements in a stalagmite from southwestern Japan: A potential proxy for chemical weathering. Geochemical Journal, 2014, 48, 73-84.	1.0	11
176	Coral record of variability in the upstream <scp>K</scp> uroshio <scp>C</scp> urrent during 1953–2004. Journal of Geophysical Research: Oceans, 2017, 122, 6936-6946.	2.6	11
177	δ18O, δ13C, elemental content and depositional features of a stalagmite from Yelang Cave reflecting climate and vegetation changes since late Pleistocene in central Guizhou, China. Quaternary International, 2017, 452, 102-115.	1.5	11
178	Highly-sensitive open-cell LA-ICPMS approaches for the quantification of rare earth elements in natural carbonates at parts-per-billion levels. Analytica Chimica Acta, 2018, 1018, 54-61.	5.4	11
179	Pinatubo Volcanic Eruption Exacerbated an Abrupt Coral Mortality Event in 1991 Summer. Geophysical Research Letters, 2018, 45, 12,396.	4.0	11
180	C-Sr-Pb isotopic characteristics of PM2.5 transported on the East-Asian continental outflows. Atmospheric Research, 2019, 223, 88-97.	4.1	11

#	Article	IF	CITATIONS
181	Fossil travertine system and its palaeofluid provenance, migration and evolution through time: Example from the geothermal area of Acquasanta Terme (Central Italy). Sedimentary Geology, 2020, 398, 105580.	2.1	11
182	Luminescence dating of Late Pleistocene faults as evidence of uplift and active tectonics in Sardinia, W Mediterranean. Terra Nova, 2020, 32, 261-271.	2.1	11
183	Measurements of natural uranium concentration and isotopic composition with permil-level precision by inductively coupled plasma-quadrupole mass spectrometry. Geochemistry, Geophysics, Geosystems, 2006, 7, n/a-n/a.	2.5	10
184	Temporal Variations of Radiocarbon Reservoir Ages in the South Pacific Ocean during the Holocene. Radiocarbon, 2015, 57, 507-515.	1.8	10
185	New precise dates for the ancient and sacred coral pyramidal tombs of <i>Leluh</i> (Kosrae,) Tj ETQq1 1 0.7843	14.rgBT /O	verlock 10 T
186	Multi-scale Holocene Asian monsoon variability deduced from a twin-stalagmite record in southwestern China. Quaternary Research, 2016, 86, 34-44.	1.7	10
187	Indian summer monsoon variability in southern India during the last deglaciation: Evidence from a high resolution stalagmite δ180 record. Palaeogeography, Palaeoclimatology, Palaeoecology, 2017, 485, 476-485.	2.3	10
188	Integrated stratigraphy of ODP Site 1115 (Solomon Sea, southwestern equatorial Pacific) over the past 3.2†Ma. Marine Micropaleontology, 2018, 144, 25-37.	1.2	10
189	Coral-inferred monsoon and biologically driven fractionation of offshore seawater rare earth elements in Beibu Gulf, northern South China Sea. Solid Earth Sciences, 2019, 4, 131-141.	1.7	10
190	Millennial-scale Asian monsoon variability during MIS 9 revealed by a high-resolution stalagmite δ180 record in Luoshui Cave, central China. Quaternary Science Reviews, 2020, 234, 106218.	3.0	10
191	Paleotemperature reconstructions using speleothem fluid inclusion analyses from Hungary. Chemical Geology, 2021, 563, 120051.	3.3	10
192	First records of syn-diagenetic non-tectonic folding in quaternary thermogene travertines caused by hydrothermal incremental veining. Tectonophysics, 2017, 700-701, 60-79.	2.2	9
193	Carbon stable isotope record in the coral species Siderastrea stellata: A link to the Suess Effect in the tropical South Atlantic Ocean. Palaeogeography, Palaeoclimatology, Palaeoecology, 2018, 497, 82-90.	2.3	9
194	A gradual transition into Greenland interstadial 14 in southeastern China based on a sub-decadally-resolved stalagmite record. Quaternary Science Reviews, 2021, 253, 106769.	3.0	9
195	Holocene sea surface temperature variations recorded in corals from Kikai Island, Japan. Geochemical Journal, 2017, 51, e9-e14.	1.0	9
196	Change of the ENSO-related δ18O–SST correlation from coral skeletons in northern South China Sea: A possible influence from the Kuroshio Current. Journal of Asian Earth Sciences, 2010, 39, 684-691.	2.3	8
197	Comparison of speleothem l̃18O records from eastern China with solar insolation, ice core and marine records: Similarities and discrepancies on different time scales. Journal of Asian Earth Sciences, 2011, 40, 1151-1163.	2.3	8
198	An abrupt backreef infilling in a Holocene reef, Paraoir, Northwestern Luzon, Philippines. Coral Reefs, 2013, 32, 293-303.	2.2	8

#	Article	IF	CITATIONS
199	Application of Kernel Density Estimates to Lead Isotope Compositions of Bronzes from Ningxia, Northâ€West China. Archaeometry, 2018, 60, 128-143.	1.3	8
200	Mantle fluids associated with crustal-scale faulting in a continental subduction setting, Taiwan. Scientific Reports, 2019, 9, 10805.	3.3	8
201	Uranium-Series Dating Of Speleothemes: Current Techniques, Limits amp; Applications. , 2007, , 177-197.		8
202	Were springline carbonates in the Kurkur–Dungul area (southern Egypt) deposited during glacial periods?. Journal of the Geological Society, 2021, 178, .	2.1	8
203	Three-phase structure of the East Asia summer monsoon during Heinrich Stadial 4 recorded in Xianyun Cave, southeastern China. Quaternary Science Reviews, 2021, 274, 107267.	3.0	8
204	Structural characteristics of an active fold-and-thrust system in the southeastern Atacama Basin, northern Chile. Tectonophysics, 2016, 685, 44-59.	2.2	7
205	The Preboreal-like Asian monsoon climate in the early last interglacial period recorded from the Dark Cave, Southwest China. Journal of Asian Earth Sciences, 2017, 143, 39-44.	2.3	7
206	Evidence for the Thermal Bleaching of <i>Porites</i> Corals From 4.0Âka B.P. in the Northern South China Sea. Journal of Geophysical Research G: Biogeosciences, 2018, 123, 79-94.	3.0	7
207	Giant tufas of Lake Van record lake-level fluctuations and climatic changes in eastern Anatolia,Turkey. Palaeogeography, Palaeoclimatology, Palaeoecology, 2019, 533, 109226.	2.3	7
208	Age of the dacite of Sunset Amphitheater, a voluminous Pleistocene tephra from Mount Rainier (USA), and implications for Cascade glacial stratigraphy. Journal of Volcanology and Geothermal Research, 2019, 376, 27-43.	2.1	7
209	Corals Reveal an Unprecedented Decrease of Arabian Sea Upwelling During the Current Warming Era. Geophysical Research Letters, 2021, 48, e2021GL092432.	4.0	7
210	Early Holocene permafrost retreat in West Siberia amplified by reorganization of westerly wind systems. Communications Earth & Environment, 2021, 2, .	6.8	7
211	Two modes of climatic control in the Holocene stalagmite record from the Japan Sea side of the Japanese islands. Island Arc, 2015, 24, 342-358.	1.1	6
212	Stalagmite δ18O variations in southern India reveal divergent trends of Indian Summer Monsoon and East Asian Summer Monsoon during the last interglacial. Quaternary International, 2015, 371, 191-196.	1.5	6
213	Coral boulders along the coast of the Lanyu Island, offshore southeastern Taiwan, as potential paleotsunami records. Journal of Asian Earth Sciences, 2015, 114, 588-600.	2.3	6
214	Climatic Constraints on Growth Rate and Geochemistry (Sr/Ca and U/Ca) of the Coral <i>Siderastrea stellata</i> in the Southwest Equatorial Atlantic (Rocas Atoll, Brazil). Geochemistry, Geophysics, Geosystems, 2018, 19, 772-786.	2.5	6
215	Variable uplift rate through time: Holocene coral reef and neotectonics of Lutao, eastern Taiwan. Journal of Asian Earth Sciences, 2018, 156, 201-206.	2.3	6
216	Sub-decadally-resolved Asian monsoon dynamics during Chinese interstadial 21 in response to northern high-latitude climate. Journal of Asian Earth Sciences, 2019, 172, 243-248.	2.3	6

#	Article	IF	CITATIONS
217	Emerged Coral Reefs Record Holocene Lowâ€Angle Normal Fault Earthquakes. Geophysical Research Letters, 2020, 47, e2020GL089301.	4.0	6
218	A detailed East Asian monsoon history of Greenland Interstadial 21 in southeastern China. Palaeogeography, Palaeoclimatology, Palaeoecology, 2020, 552, 109752.	2.3	6
219	Middle Pleistocene fluid infiltration with 10–15Âka recurrence within the seismic cycle of the active Monte Morrone Fault System (central Apennines, Italy). Tectonophysics, 2022, 827, 229269.	2.2	6
220	Stalagmite-Inferred Climate in the Western Mediterranean during the Roman Warm Period. Climate, 2022, 10, 93.	2.8	6
221	Coral-based Holocene sea level of Paraoir, western Luzon, Philippines. Journal of Asian Earth Sciences, 2016, 123, 61-66.	2.3	5
222	Evidence of solar insolation and internal forcing of sea surface temperature changes in the eastern tropical Indian Ocean during the Holocene. Quaternary International, 2018, 490, 1-9.	1.5	5
223	Late Quaternary uplift across northwest Luzon Island, Philippines constrained from emergent coral reef terraces. Earth Surface Processes and Landforms, 2018, 43, 3114-3132.	2.5	5
224	Multi-Isotope Investigations for Scientific Characterisation and Provenance Implication of Banded Travertines from Tripolis Antique City (Denizli–Turkey). Environmental Archaeology, 2019, 24, 317-336.	1.2	5
225	El Niño–Southern Oscillation and internal sea surface temperature variability in the tropical Indian Ocean since 1675. Climate of the Past, 2021, 17, 151-170.	3.4	5
226	The multidisciplinary approaches on facies developments and depositional systems of the Bahçecik travertines, G¼m¼!hane, NE-Turkey. Turkish Journal of Earth Sciences, 2021, 30, 561-579.	1.0	5
227	Mekong River discharge and the East Asian monsoon recorded by a coral geochemical record from Con Dao Island, Vietnam. Geochemical Journal, 2019, 53, e1-e7.	1.0	5
228	Role of carbon and sulfur biogeochemical cycles on the seasonal arsenic mobilization process in the shallow groundwater of the Bengal aquifer. Applied Geochemistry, 2022, 141, 105322.	3.0	5
229	Holocene surface hydroclimate changes in the Indo-Pacific warm pool. Quaternary International, 2018, 482, 1-12.	1.5	4
230	A decadal-resolution stalagmite record of strong Asian summer monsoon from northwestern Vietnam over the Dansgaard–Oeschger events 2–4. Journal of Asian Earth Sciences: X, 2020, 3, 100027.	0.9	4
231	²³⁶ U/ ²³⁸ U Analysis of Femtograms of ²³⁶ U by MC-ICPMS. Analytical Chemistry, 2021, 93, 8442-8449.	6.5	4
232	Subannual-to-biannual-resolved travertine record of Asian Summer Monsoon dynamics in the early Holocene at the eastern margin of Tibetan Plateau. Applied Geochemistry, 2022, , 105305.	3.0	4
233	Relict Pleistocene calcareous tufa of the ChlupáÄova sluj Cave, the Bohemian Karst, Czech Republic: A petrographic and geochemical record of hydrologically-driven cave evolution. Sedimentary Geology, 2019, 385, 110-125.	2.1	3
234	New evidence for the periodic bleaching and recovery of Porites corals during the mid-late Holocene in the northern South China Sea. Global and Planetary Change, 2021, 197, 103397.	3.5	3

#	Article	IF	CITATIONS
235	Stalagmite evidence for East Asian winter monsoon variability and 18O-depleted surface water in the Japan Sea during the last glacial period. Progress in Earth and Planetary Science, 2021, 8, .	3.0	3
236	Variations and significance of Mg/Sr and 87Sr/86Sr in a karst cave system in southwest China. Journal of Hydrology, 2021, 596, 126140.	5.4	3
237	Double-plunge structure of the East Asian summer monsoon during Heinrich stadial 1 recorded in Xianyun Cave, southeastern China. Quaternary Science Reviews, 2022, 282, 107442.	3.0	3
238	Mid to late 20th century freshening of the western tropical South Atlantic triggered by southward migration of the Intertropical Convergence Zone. Palaeogeography, Palaeoclimatology, Palaeoecology, 2022, 597, 111013.	2.3	3
239	Ideas and perspectives: Southwestern tropical Atlantic coral growth response to atmospheric circulation changes induced by ozone depletion in Antarctica. Biogeosciences, 2016, 13, 2379-2386.	3.3	2
240	Reply to the comment on "First records of syn-diagenetic non-tectonic folding in Quaternary thermogene travertines caused by hydrothermal incremental veining―by Billi et alii. Tectonophysics, 2017, 721, 501-512.	2.2	2
241	Late Holocene reef ecosystem baseline: Field evidence from the raised reef terraces of Kodakara and Kikai Islands, Ryukyu Islands, Japan. Quaternary International, 2017, 455, 8-17.	1.5	2
242	Assessing the growth rate of the South Atlantic coral species Mussismilia hispida (Verrill, 1902) using carbon and oxygen stable isotopes. Journal of South American Earth Sciences, 2019, 96, 102346.	1.4	2
243	Relative Sea‣evel Changes Over the Past Centuries inÂtheÂCentral Ryukyu Arc Inferred From Coral Microatolls. Journal of Geophysical Research: Solid Earth, 2020, 125, e2019JB018466.	3.4	2
244	Paleo-earthquake records of the Hengchun offshore structure, southern Taiwan, revealed by uplifted coral colonies. Tectonophysics, 2021, 817, 229049.	2.2	2
245	Last glacial temperature reconstructions using coupled isotopic analyses of fossil snails and stalagmites from archaeological caves in Okinawa, Japan. Scientific Reports, 2021, 11, 21922.	3.3	2
246	Reply to comment by Cahyarini et al. on "A snapshot of climate variability at Tahiti at 9.5 ka using a fossil coral from IODP Expedition 310― Geochemistry, Geophysics, Geosystems, 2011, 12, .	2.5	1
247	Helium Isotopic Signature of a Plate Boundary Suture in an Active Arc–Continent Collision. ACS Earth and Space Chemistry, 2020, 4, 1237-1246.	2.7	1
248	Coral boulder transport and gravel bar formation by storms in Lumaniag village, Batangas, northwestern Philippines. Geomorphology, 2021, 376, 107554.	2.6	1
249	A dataset of the mid-brunhes period at site MD05-2925, Solomon Sea: Surface-subsurface planktonic foraminifera stable C-O isotope and Mg/Ca ratios. Data in Brief, 2021, 38, 107283.	1.0	1
250	Multicentennial to millennial–scale changes in the East Asian summer monsoon during Greenland interstadial 25. Quaternary Research, 2022, 109, 195-206.	1.7	1
251	Precipitation response to Heinrich Event-3 in the northern Indochina as revealed in a high-resolution speleothem record. Journal of Asian Earth Sciences: X, 2022, 7, 100090.	0.9	1
252	Corrigendum to "Hydrothermal fluids circulation and travertine deposition in an active tectonic setting: insights from the Kamara geothermal area (western Anatolia, Turkey).―[TECTO. 680 (2016) 211–232]. Tectonophysics, 2016, 687, 268-269.	2.2	0

#	Article	IF	CITATIONS
253	Lifecycle of an Intermontane Plio-Pleistocene Fluvial Valley of the Northern Apennines: From Marine-Driven Incision to Tectonic Segmentation and Infill. Geosciences (Switzerland), 2021, 11, 141.	2.2	0
254	Stalagmite-inferred European westerly drift in the early Weichselian with centennial-scale variability in marine isotope stage 5a. Quaternary Science Reviews, 2022, 288, 107581.	3.0	0